doi:10.3788/gzxb20164505.0523002

波长选择性平行耦合微环谐振四端口光路由

李翠婷,郑文雪,郑传涛,张大明,王一丁,马春生

(集成光电子学国家重点联合实验室吉林大学实验区,吉林大学电子科学与工程学院,长春 130012)

摘　要:利用四个平行耦合单环谐振器作为基本路由单元,数值模拟了一种可路由三种信道波长的四端口光路由器.为了实现单模传输、低传输损耗以及微环波导和信道波导的相位匹配,优化了基本路由单元的结构参量.给出了路由器的器件架构和设计方法,计算了链路光谱、插入损耗、串扰等路由特性.在选定的三个信道波长(1 550、1 551.6、1 553.2 nm)下,器件沿不同路径的插入损耗范围为0.02～0.6 dB,器件串扰的范围为−23.41～−37.71 dB.与具有相同波导参量的基于交叉耦合双环谐振器的四端口光路由器相比,该四端口光路由器在串扰和波长选择性方面略显不足,但其使用的微环数量由8个降低为4个,插入损耗由1.62 dB降低为0.02 dB.

关键词:路由器;数值模拟;波导;聚合物;插入损耗;串扰

中图分类号:TN253　　**文献标识码**:A　　**文章编号**:1004-4213(2016)05-0523002-7

Wavelength-routed Four-port Optical Router Based on Parallel-coupled Microring Resonators

LI Cui-ting, ZHENG Wen-xue, ZHENG Chuan-tao, ZHANG Da-ming, WANG Yi-ding, MA Chun-sheng

(*State Key Laboratory on Integrated Optoelectronics, College of Electronic Science and Engineering, Jilin University, Changchun, 130012, China*)

Abstract: By adopting four parallel-coupling one microring resonator as basic routing elements, a kind of four-port optical router is proposed, which can passively route three channel wavelengths. The structural parameters of the routing element were optimized for single-mode transmission, low optical loss and phase-match between microring waveguide and channel waveguide. The device architecture as well as design scheme of the router was presented, and routing characteristic including spectrum characteristic, insertion loss and crosstalk were calculated. Under the selected three channel wavelengths of 1 550, 1 551.6 and 1 553.2 nm, the insertion losses along all routing paths are within 0.02～0.6 dB, and the crosstalk ranges from −23.41 to −37.71 dB. Compared with the previously reported four-port optical router using cross-coupling two microring resonator and the same waveguide parameters, the proposed router reveals slightly higher crosstalk and inferior spectral selectivity, but it does show smaller insertion loss (decreasing from 1.62 dB to 0.02 dB) and uses less rings (decreasing from 8 to 4).

Key words: Router; Numerical simulation; Waveguide; Polymer; Insertion loss; Crosstalk

OCIS Codes: 230.0230; 230.3120; 230.7370

Foundation item: The National Science Foundation Council of China (Nos. 61107021, 61177027), the Ministry of Education of China (Nos. 20110061120052, 20120061130008), the China Postdoctoral Science Foundation Funded Project (Nos. 20110491299, 2012T50297), the Science and Technology Department of Jilin Province of China (No. 20130522161JH), and the Special Funds of Basic Science and Technology of Jilin University (No. 201103076)

First author: LI Cui-ting (1991−), female, master candidate, mainly focuses on optical waveguide devices. Email: lict14@mails.jlu.edu.cn

Supervisor(Contact author): ZHENG Chuan-tao(1982−), male, associate professor, mainly focuses on optoelectronic device and system. Email: zhengchuantao@jlu.edu.cn

Received: Nov. 2, 2015; **Accepted**: Dec. 21, 2015

0 Introduction

In on-chip multi-core processor systems, Optical Networks-on-chip (ONoC) is an effective method to increase transmission bandwidth, decrease time delay, and reduce power consumption[1-3]. One of the key components in ONoC is optical router [4-6], which is composed of waveguides and optical switches. Generally, the structure of the router is based on the topology of the photonic NoC. For example, Mesh photonic NoC requires 4-, 5- and 6-port optical routers, while Fat-Tree photonic NoC only require 4-port optical router. Therefore, several kinds of 4- and 5-port optical routers based on Microring Resonator (MRR) optical switches or Mach-Zehnder (MZ) optical switches have been proposed or even experimentally demonstrated.

Within the available switching structures, MRR are typically preferred due to their ultra-compact size, simple-mode resonances, and ease of phase-matching between an MRR and its coupling waveguides. Consequently, by utilizing MRR as the basic switching element, both active and passive optical routers have been constructed with different topologies, e. g., the non-blocking four-port optical router[7], a reconfigurable non-blocking four-port optical router based on microring resonators tuned through thermo-optic effect[8], the 1-stage four-port optical router with high scalability[9], polymeric N-stage cascaded five-port optical router[10], the 8-port optical router with scalable 7N channel wavelengths[11], and the universal N-port nonblocking optical router[12].

Previously, a 1-stage four-port optical router was reported by our group based on four channel waveguides and 8 microrings with two kinds of radiuses[9]. In order to decrease the number of the used microrings as well as to maintain the same routing function, we propose a kind of four-port optical router using only 4 microrings. Because of the simplified routing structure, the fabrication and control of the router can be easier than the device reported in Ref. [9]. Also, the proposed router reveals smaller insertion loss.

1 Basic 2×2 MRR routing elements

The Parallel-Coupling One Microring Resonator (PCO-MRR) element structure is shown in Fig. 1, which consists of two horizontal channel waveguides and one microring coupled with the two channel waveguides. For obtaining the same mode propagation constants, the two core widths of MRR waveguide and channel waveguide are slightly different. Considering the symmetry of the PCO-MRR, here only analyze the case of light inputting into the left port, e. g. $a_{11}\neq 0$ and $a_{22}=0$. As shown in Fig. 1, at the coupling plane between the microring R and the upper channel, a_{11}, b_{11} (a_{22}, b_{22}) and a_{21}, b_{21} (a_{12}, b_{12}) are the input and output light amplitudes of the upper channel waveguide and microring waveguide, respectively. Define t and κ as the transmission coefficient and the coupling coefficient between the MRR waveguide and the channel waveguide, respectively. Based on resonance theory, the amplitude transfer function of the basic routing element is obtained by

$$U_{\mathrm{PCO}}^{\mathrm{t}}=\frac{b_{11}}{a_{11}}=\frac{b_{22}}{a_{22}}=\frac{t[1-\exp(-\mathrm{j}2\phi)]}{1-t^2\exp(-\mathrm{j}2\phi)} \tag{1}$$

$$V_{\mathrm{PCO}}^{\mathrm{d}}=\frac{b_{22}}{a_{11}}=\frac{b_{11}}{a_{22}}=\frac{-\kappa^2\exp(-\mathrm{j}\phi)}{1-t^2\exp(-\mathrm{j}2\phi)} \tag{2}$$

where $\phi=\pi R(\beta_{\mathrm{R}}-\mathrm{j}\alpha_{\mathrm{R}})$, $\beta_{\mathrm{R}}=(2\pi/\lambda)n_{\mathrm{R}}$ is the mode propagation constants of the MRR waveguide, which should be approximately equal for phase matching, α_{R} is the mode amplitude loss coefficients of the MRR waveguide. In Eqs. (1)~(2), the superscripts "t" and "d" represent "through-state" and "drop-state", respectively. Then the wavelength-dependent output powers from the through-port and drop-port can be expressed as

$$P_{\mathrm{t}}^{\mathrm{PCO}}(\lambda)=10\log_{10}(|U_{\mathrm{PCO}}^{\mathrm{t}}|^2) \tag{3}$$

$$P_{\mathrm{d}}^{\mathrm{PCO}}(\lambda)=10\log_{10}(|V_{\mathrm{PCO}}^{\mathrm{d}}|^2) \tag{4}$$

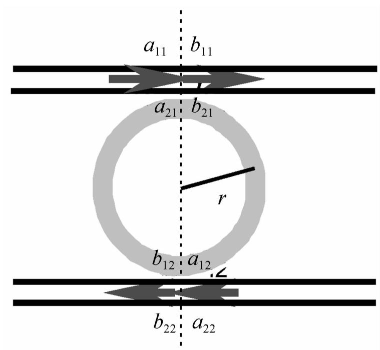

Fig. 1 The structure of proposed PCO-MRR

The waveguide cross-section between MRR waveguide and channel waveguide are shown in Fig. 2. Around 1 550 nm, the refractive index n_{10} of the polymeric waveguide core is 1.590 and the bulk amplitude attenuation coefficient $\alpha_{10}=0.25$ dB/cm[13-14]; the refractive index n_{20} of the polymer buffer layer is 1.461, and its bulk amplitude attenuation coefficient is $\alpha_{10}=0.25$ dB/cm[15]; the refractive index n_{30} of the left/right cladding (air) is 1.000 and the bulk amplitude attenuation coefficient $\alpha_{30}=0$. In the design, E_{00}^{y} is selected as the fundamental propagation mode. Without considering bending effect of MRR waveguide, the mode characteristics of the rectangular waveguide can be analyzed by using the theoretical approach proposed in Ref. [16]; under the case of considering bending effect, those of the curved rectangular waveguide can be analyzed with the numerical approach proposed in Ref. [17]. The values of the selected structural parameters as well as those of some characteristic parameters are listed in Table 1, which will be used in the performances' estimation of the three routers.

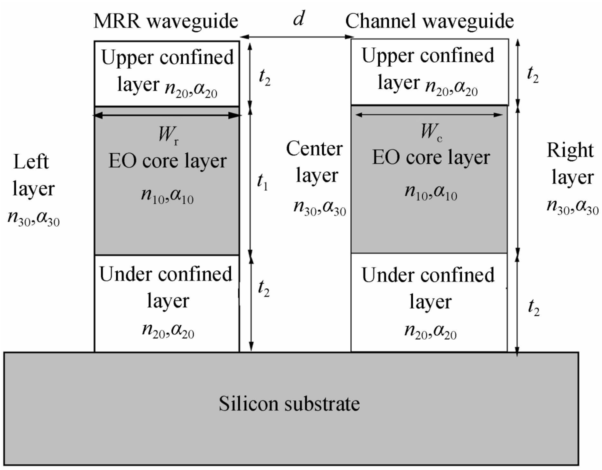

Fig. 2 Waveguide cross-section view between MRR waveguide and channel waveguide

Table 1 Optimized parameters of the basic routing elements

Parameters	Value	Parameters	Value
Core thickness t_1	1.7 μm	Transmittance coefficient t (@1 550 nm)	0.99622
Core width w_c	2.03 μm	Coupling coefficient κ(@1 550 nm)	0.08684
Core width w_r	1.7 μm	Mode effective index n_C (@1 550 nm)	1.5243
Buffer thickness t_2	2.5 μm	Mode effective index n_R (@1 550 nm)	1.5243
Coupling gap d	0.14 μm	Amplitude loss coefficient α_R (@1 550 nm)	0.25614 dB/cm
Resonance order m	85	Three routing wavelengths $\lambda_{1,2,3}$	1 550.0, 1 551.6, 1 553.2 nm

2 Four-port optical router

The structure model of the PCO-MRR-based four-port polymer optical router is shown in Fig. 3, which consists of eight straight waveguides, four bending waveguides, and four groups of PCO-MRR with two kinds of ring radiuses. The lengths of the input and output waveguides of each port are $L_1 = 100$ μm, and the center to center distance between two neighboring rings is $L_2 = 100$ μm. Four circular bending waveguides are adopted in the topology, their bending radiuses are $R = L_2 - [r_1 + r_2 + 2(w_r/2 + d + w_c)] = 66.432$ μm, and their waveguide lengths are $L_3 = 0.5\pi R = 104.298$ μm.

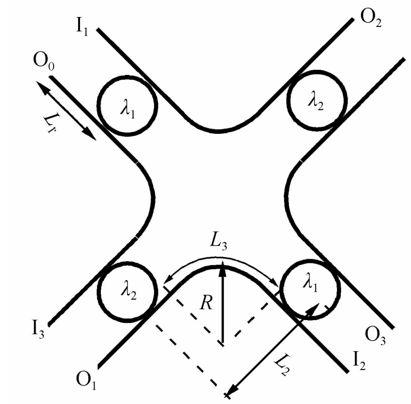

Fig. 3 The structure model of the PCO-MRR-based four-port polymer optical router

The four-port optical routers is operated at three kinds of wavelengths, i.e. 1 550, 1 551.6 and 1 553.2 nm, and it requires two kinds of basic routing elements, numbered by #1 (resonance at 1 550 nm) and #2 (resonance at 1 551.6 nm), respectively. For convenience, define the channels with the wavelengths of 1 550, 1 551.6 and 1 553.2 nm as channel #1, #2 and #3, respectively. The two ring radiuses and the routing wavelengths should satisfy the resonance equation $2\pi R n_R = m\lambda$, where m is resonance order. Use the same theory in Refs. [10-11], the resonance wavelengths and the corresponding bending radiuses of the two kinds of microrings are taken as those listed in Table 2. When three light signals with wavelengths of λ_1, λ_2, and λ_3 input into one certain port simultaneously, they will output from their own appointed port, which is called definite-path routing. For example, when the hybrid signal input into port I_0, according to the routing path obtained from Fig. 3, the three wavelength signals will output from port O_1, O_2, and O_3, respectively. Similarly, the situations of optical signals injecting into ports I_1, I_2 and I_3 can be analyzed. The total possible definite-path routing links are shown in Table 3, which illustrates that the optical

Table 2 The three selected routing wavelengths and two ring radiuses

Channel number	Channel wavelength/nm	Ring radius/μm	Mode effective index
1	λ_1 = 1 550.0	13.756	1.524 31
2	λ_2 = 1 551.6	13.772	1.524 15
3	λ_3 = 1 553.2	/	/

Table 3 Routing paths of the four-port optical router

Input	Output			
	O_0	O_1	O_2	O_3
I_0	/	λ_1	λ_2	λ_3
I_1	λ_1	/	λ_3	λ_2
I_2	λ_2	λ_3	/	λ_1
I_3	λ_3	λ_2	λ_1	/

Table 4 Operation states of the PCO-MRR-based optical router

Routing states		Input			
		I_0	I_1	I_2	I_3
Single-wavelength routing (output port, wavelength)	1	O_1, λ_1	O_0, λ_1	O_3, λ_1	O_2, λ_1
	2	O_3, λ_3	O_0, λ_1	O_1, λ_3	O_2, λ_3
	3	O_1, λ_1	O_3, λ_2	O_0, λ_2	O_2, λ_1
	4	O_2, λ_2	O_0, λ_1	O_3, λ_1	O_1, λ_2
	5	O_1, λ_1	O_2, λ_3	O_3, λ_1	O_0, λ_3
	6	O_3, λ_3	O_2, λ_3	O_1, λ_3	O_0, λ_3
	7	O_2, λ_2	O_3, λ_2	O_0, λ_2	O_1, λ_2
	8	O_3, λ_3	O_2, λ_3	O_0, λ_2	O_1, λ_2
	9	O_2, λ_2	O_3, λ_2	O_1, λ_3	O_0, λ_3
Multi-wavelength routing (output ports, wavelengths)	10	O_1, O_2, O_3 $\lambda_1 \lambda_2, \lambda_3$	/	/	/
	11	/	O_0, O_3, O_2 $\lambda_1 \lambda_2, \lambda_3$	/	/
	12	/	/	O_3, O_0, O_1 $\lambda_1 \lambda_2, \lambda_3$	/
	13	/	/	/	O_2, O_1, O_0 $\lambda_1 \lambda_2, \lambda_3$

signal with wavelength of $\lambda_i (i=1, 2, 3)$ has a specific input-output path selected by microring routing elements.

The non-blocking topology needs to avoid two packets of signals that are destined for the same output as well as signals that enter and exit from the same port (U-turn). So the number of routing states is 13, as shown in Table 4. Notice that when the device works at states 10 to 13, broadcasting routing mode is established. Each of the four ports in this device is able to not only receive broadcasting information from the other three ports but also broadcast messages to them. In this working state, no signal is allowed to be sent into the other three input ports, otherwise there will be signal contention at output port to cause the undesired blocking.

3 Characteristics analysis

3.1 Transmission characteristics of the routing elements

Using the amplitude transfer function of the basic routing element, at the two output ports (defined as drop-port and through-port) of the basic routing elements (resonance at 1 550 and 1 551.6 nm), the curves of output powers versus wavelength are shown in Figs. 4(a)~(b), respectively. For the convenience in the following analysis, define loss parameters as follows: when the light with wavelength λ_j inputs into the basic routing element with resonance wavelength λ_i, define $IL_{\lambda_i}^{\lambda_j,\mathrm{on}}$ as the insertion loss of the on-port with the maximum output power, and $IL_{\lambda_i}^{\lambda_j,\mathrm{off}}$ is that of the off-port with the minimum output power. Because of the symmetry of this structure, there are 12 loss parameters totally, and their values are listed in Table 5 according to the calculation results in Figs. 4(a) and (b).

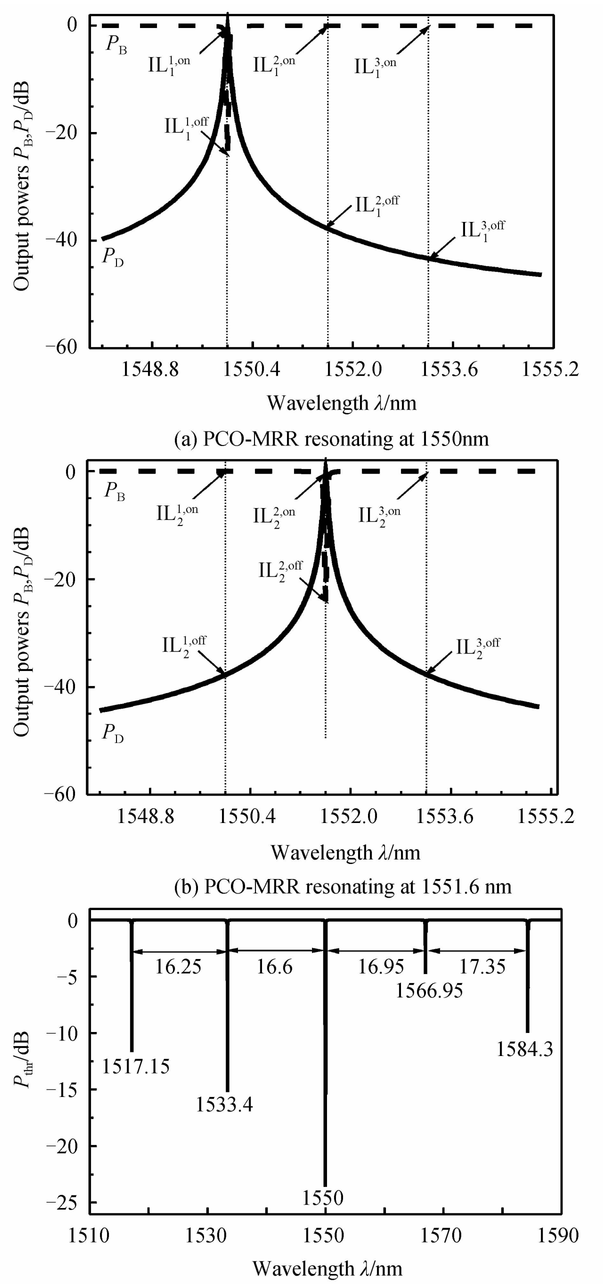

(a) PCO-MRR resonating at 1550nm

(b) PCO-MRR resonating at 1551.6 nm

(c) FSR

Fig. 4 Spectral characteristics and FSR of the PCO-MRR

As exhibited in Fig. 4(c), the Free Spectral Range (FSR) of the PCO-MRR is about 16 nm, and the three channel wavelengths are within the same FSR region.

Table 5 Loss parameters of the two basic routing elements for PCO-MRR at the three channel wavelengths under on and off states

		Channel wavelength number j					
		1,on	1,off	2,on	2,off	3,on	3,off
Rouging Element i	1	0.5670	23.9871	0.0008	37.7776	0.0002	43.3438
	2	0.0008	37.7983	0.5618	24.0634	0.0008	37.6785

Note: the unit of loss in this table is dB.

3.2 Output spectrum

When a channel wavelength λ_k inputs into port I_i, it will output from an appointed port O_j ($i \neq j$), and denote the routing path by l_i^{j,λ_k}. The routing path from input port I_i to output port O_i is selected as the path with the nearest propagation distance, marked by l_i^i. During the propagation of a light with wavelength λ from input port I_i to output port O_j, along the definite routing path l_i^j, it will pass through several basic routing elements (drop-state or through-state) and definitely long channel waveguide (the length is denoted by L_i^j), and for the basic routing unit with resonance wavelength λ_k ($k=1\sim2$), assume there are totally m_k drop-states (output power is characterized by $P_d^{\lambda_k}$) and n_k through-states (output power is characterized by $P_t^{\lambda_k}$). Therefore, the output powers in dB form can be expressed as

$$P_i^j(\lambda) = -L_i^j \cdot 2\alpha_C(\lambda) + \sum_{k=1}^{2}\left[m_k P_d^{\lambda_k}(\lambda) + n_k P_t^{\lambda_k}(\lambda)\right] \tag{5}$$

For the router, using Eq. (5), along each path, the output spectrums of all output ports relative to each input port are calculated and shown in Fig. 5. In the figure, the four sub-figures in row i ($i=0\sim3$) show the spectrums of the four output ports when the light inputs into port I_i.

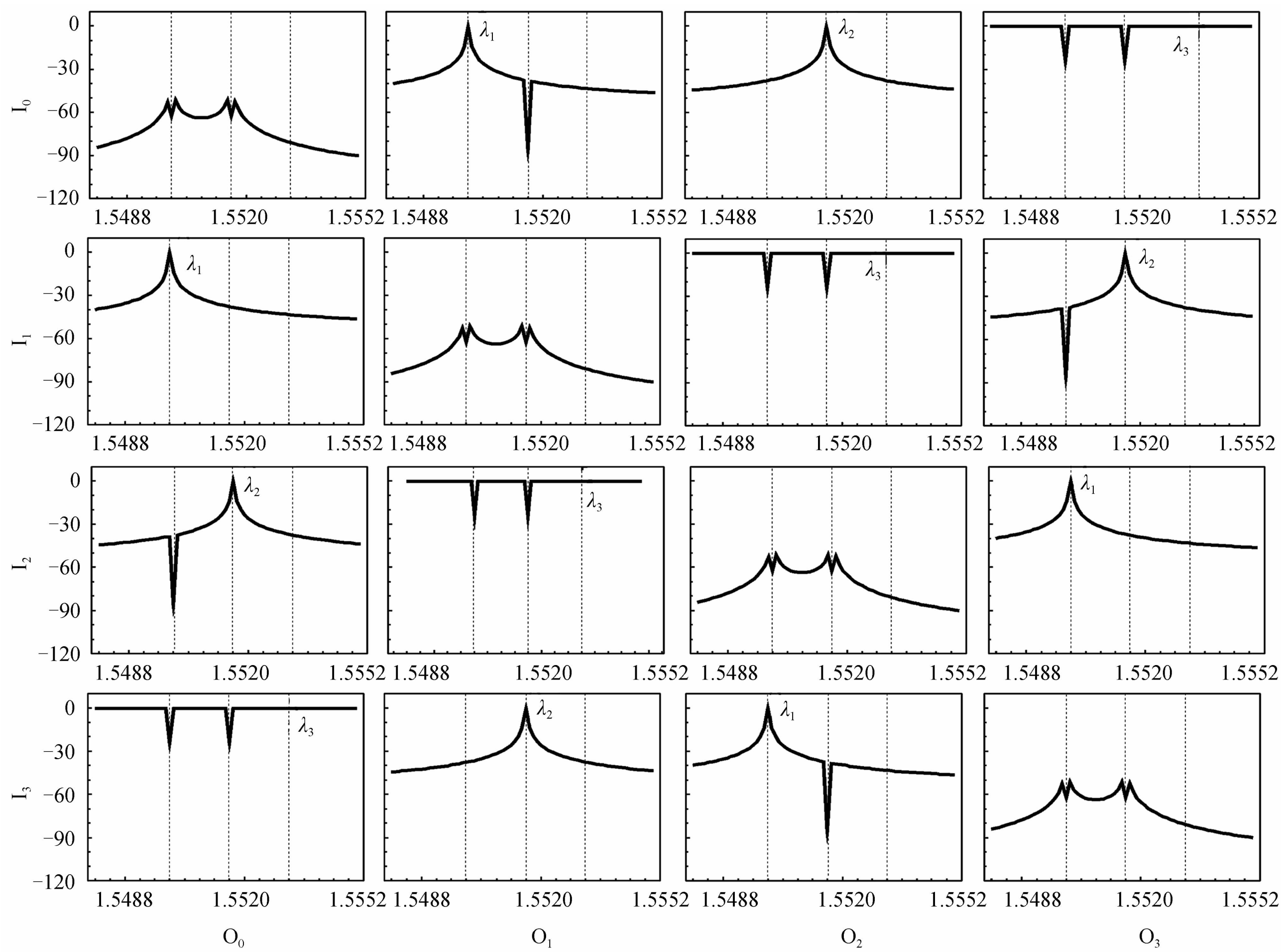

Fig. 5 Optical spectra responses of the four-port optical router under different input/output routing operations

3.3 Insertion loss and crosstalk

Insertion loss is intrinsic characteristics of photonic devices. Optical signal with wavelength of λ_i ($i=1, 2, 3$) has a specific input-output routing path, and in this case, the ratio between output power and input power is defined as the insertion loss (in dB form). Assume that P_i^{j,λ_k} is the output power at port j (the input power into port i is assumed to be 0 dB (1mW) at the wavelength of λ_k), then the loss at the port with the maximum output power is defined as the insertion loss of input light with this wavelength, i. e.

$$IL_i^{\lambda_k} = -1 \times P_i^{j^*,\lambda_k} \tag{6}$$

with

$$P_i^{j^*,\lambda_k} = \max_j P_i^{j,\lambda_k} \tag{7}$$

As long as the output power is obtained, the insertion loss can be calculated. On the basis of the symmetry between the two ports of I_0 and I_3 and that between the two ports of I_1 and I_2, with the same input wavelength, the identical insertion loss and crosstalk are derived for the corresponding output ports. With the defined loss parameters in Table 5, the insertion losses of each wavelength signal under the case of light inputting into different ports can be directly obtained, as depicted in Fig. 4. It can be found that, the maximum insertion loss of all channel wavelengths is 0.59 dB and minimum insertion loss is 0.02 dB.

Although the router can establish and maintain optical path from one source to the corresponding destination for definite optical signal, a major shortcoming of the optical router is crosstalk, which is caused by the effect of the undesirable coupling between the waveguide and rings of the basic elements used in the optical router. The crosstalk will be defined as the power subtraction between the maximum output power of all off-ports and the output power of on-port, i.e. when the light with wavelength of λ_k inputs into port I_i, it can be obtained that

$$CT_i^{\lambda_k} = \max_{j,j\neq j^*} P_i^{j,\lambda_k} - P_i^{j^*,\lambda_k} \tag{8}$$

Fig. 6 also shows the four-port optical router's crosstalk of all channel wavelengths under the cases of lightwave signals inputting into different ports. When the three lightwave signals (λ_1, λ_2, λ_3) input into port I_0 or I_3, the crosstalk of the three channel wavelengths are −23.41, −23.48 and −37.70 dB, respectively. As shown in Fig. 6(b), when the three lightwave signals (λ_1, λ_2, λ_3) input into port I_1 or I_2, the

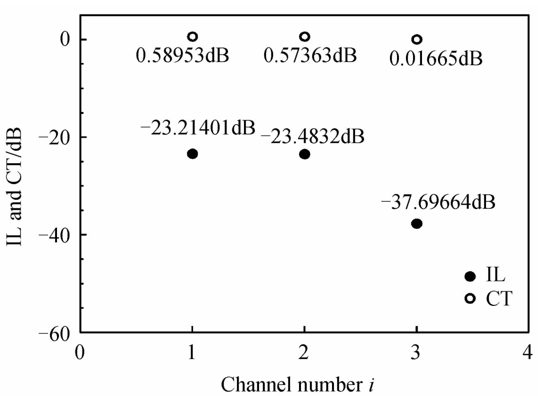

(a) Light is launching into ports I_0 or I_3

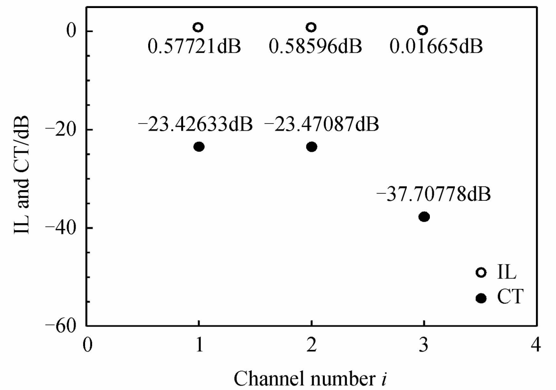

(b) Light is launching into ports I_1 or I_2

Fig. 6 For the four-port optical router, the insertion losses of definite routing port under on state and the maximum crosstalk of this on-port relative to other off-ports

crosstalk are −23.43, −23.47 and −37.71 dB, respectively.

4 Comparison

Previously, a four-port optical router was reported based on four Cross Coupling two Microring Resonators (CCO-MRRs)[18]. Since the two routers have the same routing operation, we made a comparison between them directly. Here, based on the same waveguide structure and parameters, we calculate its insertion loss and crosstalk and compare them with those of the device in this paper, as listed in Table 6. The device CCT-MRR is based on the structure reported in Ref. [15]. It can be seen from the table that, the two routers have the same number of waveguides, the same number of routing elements, and the same species of routing element; the PCO-MRR-based router has no waveguide crossing, while the other router have 4 waveguide crossings; the used MRR number of PCO-MRR-based router (4 rings) are half of that of the CCT-MRR-based router (8 rings); the PCO-MRR-based router depicts smaller insertion loss (0.02~0.6 dB). However, the four-port optical router proposed in this paper shows slightly larger crosstalk (<−23 dB) than that the CCT-MRR-based router (<−39 dB). Also, the CCT-MRR-based router has better spectral selectivity than this device due to the use of two-resonator cross-coupling structure.

Table 6 Comparison results of the two four-port optical routers

4-port router	Waveguide		Routing element		Ring number	Insertion loss/dB	Crosstalk /dB	Spectral selectivity
	No.	Cross	No.	Species				
CCT-MRR	4	4	4	2	8	1.62~2.21	<−39	Good
PCO-MRR	4	0	4	2	4	0.02~0.59	<−23	General

5 Conclusion

In conclusion, a kind of four-port optical router is proposed. The structural parameters of the basic routing elements are optimized, and the routing topology of the router is presented. Then the four-port optical router's characteristic parameters like spectrum characteristic, insertion loss, and crosstalk are calculated using the MATLAB program. The router only uses 4 rings and has 12 definite routing paths. The maximum insertion loss of all channel wavelengths is 0.59 dB and minimum insertion loss is 0.02 dB, and the crosstalk ranges from −23.41 to −37.71. The proposed optimization theory and method are of well meanings in the design of optical routers with similar structure.

References

[1] SHACHAM A, BERGMAN K, CARLONI L P. Photonic networks-on-chip for future generations of chip multiprocessors [J]. *IEEE Transactions on Computers*, 2008, **57**(9): 1246-1260.

[2] BEAUSOLEIL R G, KUEKES P J, SNIDER G S, *et al*. Nanoelectronic and nanophotonic interconnect[C]. Proceedings of the IEEE, 2008, **96**(2): 230-247.

[3] AHN J, FIORENTINO M, BEAUSOLEIL R G, *et al*. Devices and architectures for photonic chip-scale integration [J]. *Applied Physics A*, 2009, **95**(4): 989-997.

[4] TAN Xian-fang, YANG Mei, ZHANG Lei, *et al*. A generic optical router design for photonic network-on-chips [J]. *Journal of Lightwave Technology*, 2012, **30**(3): 368-376.

[5] BIBERMAN A, LEE B G, SHERWOOD-DROZ N, *et al*. Broadband operation of nanophotonic router for silicon photonic networks-on-chip[J]. *IEEE Photonics Technology Letters*, 2012, **22**(12): 926-928.

[6] GU Hua-xi, MO K H, XU Jiang, *et al*. A low-power low-cost optical router for optical networks-on-chip in multiprocessor systems-on-chip [C]. Proceedings IEEE Computer Society Annual Symposium on VLSI, 2009, 19-24.

[7] JI Rui-qiang, YANG Lin, ZHANG Lei, *et al*. Microring-resonator-based four-port optical router for photonic networks-on-chip[J]. *Optics Express*, 2011, **19**(20): 18945-18955.

[8] YANG Lin, JIA Hao, ZHAO Yun-chou, *et al*. Reconfigurable non-blocking four-port optical router based on microring resonators[J]. *Optics Letters*, 2015, **40**(6): 1129-1132.

[9] LUO Qian-qian, ZHENG Chuan-tao, HUANG Xiao-liang, *et al*. Polymeric N-stage serial-cascaded four-port optical router with scalable 3N channel wavelengths for wideband signal routing application [J]. *Optical and Quantum Electronics*, 2014, **46**(6): 829-849.

[10] ZHENG Chuan-tao, LUO Qian-qian, MA Chun-sheng, *et al*. Polymeric N-stage cascaded five-port optical router with scalable 4N channel wavelengths for wideband signal routing [J]. *Optics Communications*, 2014, **322**: 214-223.

[11] LI Cui-ting, ZHENG Chuan-tao, ZHENG Yue, *et al*. Topology and investigation of a polymer 8-port optical router with scalable 7N channel wavelengths using N-stage cascading structure [J]. *Optics Communications*, 2015, **339**: 94-107.

[12] MIN Rui, JI Rui-qiang, CHEN Qiao-shan, *et al*. A universal method for constructing N-port nonblocking optical router for photonic networks-on-Chip [J]. *Journal of Lightwave Technology*, 2012, **30**(23): 3736-3741.

[13] XU Guo-yang, LIU Zhi-fu, MA Jing, *et al*. Organic electro-optic modulator using transparent conducting oxides as electrodes[J]. *Optics Express*, 2005, **13**(19): 7380-7385.

[14] LUO Jing-dong, LIU Sen, HALLER M A, *et al*. Recent progress in developing highly efficient and thermally stable nonlinear optical polymers for electro-optics [C]. Conference on Organic Photonic Materials and Devices VI, 2004, 5351: 36-43.

[15] PITOIS C, VUKMIROVIC S, HULT A, *et al*. Low-loss passive optical waveguides based on photosensitive poly (pentafluorostyrene-co-glycidyl methacrylate) [J]. *Macromolecules*, 1999, **32**(9): 2903-2909.

[16] MARCATILIE A J. Dielectric rectangular waveguide and directional coupler for integrated optics [J]. *Bell System Technology Journal*, 1969, **48**(7): 2071-2102.

[17] MELLONI A, CARNIEL F, COSTA R, *et al*. Determination of bend mode characteristics in dielectric waveguides[J]. *Journal of Lightwave Technology*, 2001, **19**(4): 571-577.

[18] LUO Qian-qian, HUANG Xiao-liang, ZHENG Chuan-tao, *et al*. Optimization of a polymer four-port microring optical router with three channel waveguides [J]. *Optoelectronics Letters*, 2015, **10**: 91-95.